Filter-aided extracellular vesicle enrichment (FAEVEr)

Jarne Pauwels[1,2], Tessa Van de Steene[1,2], Jana Van de Velde[1,2,3], Sven Eyckerman[1,2] & Kris Gevaert[1,2,$]

[1]VIB-UGent Center for Medical Biotechnology, VIB, 9052 Ghent, Belgium

[2]Department of Biomolecular Medicine, Ghent University, 9052 Ghent, Belgium

[3]Eurofins Scientific, 9052 Gent, Belgium

[$]Corresponding author: Prof. Dr. Kris Gevaert, VIB-UGent Center for Medical Biotechnology and Department of Biomolecular Medicine, Ghent University, Technologiepark-Zwijnaarde 75, 9052 Ghent, Belgium; e-mail: kris.gevaert@vib-ugent.be

ORCID ID JP: 0000-0002-8525-7109

ORCID ID TVDS: 0000-0001-7915-2055

ORCID ID SE: 0000-0001-7525-0096

ORCID ID KG: 0000-0002-4237-0283

A. Abstract

Extracellular vesicles (EVs), membrane-delimited nanovesicles that are secreted by cells into the extracellular environment, are gaining substantial interest due to their involvement in cellular homeostasis and their contribution to disease pathology. The latter in particular has led to an exponential increase in interest in EVs as they are considered to be circulating packages containing potential biomarkers and are also a possible biological means to deliver drugs in a cell-specific manner. However, several challenges hamper straightforward analysis of EVs as they are generally low abundant and reside in complex biological matrices. These matrices typically contain protein concentrations that vastly exceed those of the EV proteome and contain particles in the same size and density range (e.g. protein aggregates and apolipoprotein particles). Therefore, extensive EV isolation and purification protocols are imperative and many have been developed, including (density) ultracentrifugation, size-exclusion and precipitation methods. Here, we describe an approach based on 300 kDa MWCO filtration, which allows processing of multiple samples in parallel within a reasonable timeframe and at moderate cost. We demonstrate that our strategy is capable of quantitatively retaining EV particles on filters, whilst allowing extensive washing with relatively high percentages of the mild detergent TWEEN-20. In addition, we provide evidence that the retained EVs can be recuperated from the filter for qualitative studies or can be directly lysed on the filter for the recovery of the EV protein cargo for proteome analysis. Applying this strategy on MCF7 conditioned medium using different percentages of serum, we observed dramatic changes in the EV proteome.

B. Keywords

300 kDa MWCO ultrafiltration, conditioned medium, starvation, EV-depleted serum, TWEEN-20, LC-MS/MS

C. Introduction

Extracellular vesicles (EVs) are defined as the population of membrane-enclosed particles that are released by virtually all cells into their extracellular (EC) environment or into body fluids such as plasma, cerebrospinal fluid (CSF) and urine. EVs are subdivided in three major types depending on their biogenesis pathway and size. The smallest EVs, termed exosomes, are generated by invaginations at the early endosomal membrane in an endosomal-sorting complex required for transport (ESCRT) dependent [1] or in an ESCRT independent [2] manner. After scission of the invaginations, the endosomes are transformed into multivesicular bodies (MVBs), containing multiple membrane-delineated vesicles or intraluminal vesicles (ILVs). Once MVBs fuse with the plasma membrane (PM), ILVs are released in the EC environment as exosomes. Microvesicles are formed by direct outward budding of the PM followed by pinching, which is mediated by the ESCRT machinery [3]. Finally, apoptotic bodies are formed during apoptotic cell disassembly with large extrusions at the PM, fragmenting dying cells in large blobs that may even contain organelles [4]. Once released, the EVs become part of a heterogeneous pool from which the subtypes cannot be easily distinguished, resulting in the loss of biogenesis-related information. Therefore, in practice, EVs are distinguished from one another by their diameter, subdividing them in small (< 150 nm, mainly exosomes), intermediate (150 – 300 nm) and large EVs (> 300 nm) [5]. However, as there is a relatively high overlap in diameter distribution between these subclasses, no strict consensus exists [1, 6, 7].

EV biogenesis leads to two important biophysical features. First, EVs are delineated by a phospholipid bilayer that effectively shields their cargo from the EC environment, thereby increasing its stability. In addition, the EV membrane proteins and surface-associated proteins allow EVs to specifically

interact with target cells, enabling directed cargo delivery or signal transduction to distant cells, tissues and organs [8, 9]. Second, during their formation, EVs are packed with different biomolecules, including oligonucleotides (DNA and RNA), proteins, lipids and metabolites. This cargo represents a molecular snapshot of the parental cell at the moment of EV formation. In physiological conditions, this cargo takes part in cellular communication [10] and homeostasis [11, 12]. In disease, however, EV cargo can contribute to the pathology, for example by initiating pre-metastatic niches at distant locations during cancer progression [13].

Both EV characteristics are appealing for clinical implementations, for both therapeutic applications (i.e. targeted drug delivery) as well as for biomarker discovery (i.e. disease diagnosis, prognosis and therapy guidance). Although therapeutic applications remain rather hypothetical or, at best, experimental to date [14], the past decade has witnessed exponential advancements in revealing the remarkable biomarker potential of EVs. Biofluids are readily available and require low to non-invasive techniques for their isolation (e.g. plasma and urine), explaining their use as an EV source for research purposes. In general, identification of biomarkers in or on circulating EVs might lead to disease diagnosis, monitoring of disease progression and therapeutic response, all critical for optimizing precision treatments. In this respect, EVs have shown clinical potential as a source of circulating biomarkers for different cancers (e.g. breast [15], urinary tract [16] and bone cancer [17]) and other diseases such as Alzheimer's disease [18], chronic liver disease [19] and multiple sclerosis [20].

Unfortunately, there are some pressing challenges in EV research. EVs reside in complex biological matrices such as plasma and urine, and such biofluids contain proteins at levels that exceed those of the EV proteins by several orders of magnitude [21], such as albumin in plasma and uromodulin in urine. As a result, low abundant EV proteins are difficult to detect given the competitive and stochastic nature of bottom-up mass spectrometry, which is still the method-of-choice for unbiased protein biomarker

discovery. In addition, biofluids often contain particles (e.g. lipoprotein particles) that overlap in size and density with EVs, making purification of EVs challenging. Different techniques have been developed to enrich and concentrate EVs, and sometimes a combination of such techniques is used [22]. The most prominent techniques are based on EV size (ultra-centrifugation and size-exclusion [23]), density (density gradient centrifugation [24]), precipitation [25, 26] or exploitation of molecular markers on the EV surface (immune-capture approaches [27]). To further increase EV purity, especially concerning contaminating lipoprotein particles, orthogonal techniques can be combined [28]. However, a standardized approach has yet to be established as the current strategies not only differ in the consumption of resources and time, but also in terms of effectiveness and reproducibility. Indeed, the different EV isolation techniques introduce variation between experiments in terms of EV count and heterogeneity of molecular cargo [29]. This has been emphasized in different studies in which EV enrichment strategies were compared [30-33]. Along this line, initiatives such as EV-TRACK [34] and MISEV [35] were established within the EV research community to encourage transparency on experimental procedures used to enrich EVs and on acquired results, thereby supporting inter-lab reproducibility. Of interest, purified, recombinant EVs can be used as biological reference material to monitor technique development and reproducibility, and improve data normalization [6]. However, the multitude of EV enrichment techniques have one major bottleneck in common as they all lack the possibility for parallelization and high-throughput setups.

Ultrafiltration has thus far been predominantly used as an intermediate EV concentration step, either before EV isolation to reduce the volume of conditioned media [36] or liquid biopsies [37], or after EV isolation (e.g. size-exclusion fractions [38]). The main challenges when filtering complex mixtures are potential filter blocking, inefficient removal of non-EV proteins trapped on the filter and low recovery of retained EVs [39, 40]. On the other hand, ultrafiltration has little to no bias towards selecting or losing EV subpopulations [41]. In addition, ultrafiltration is rather inexpensive and fast, and thus allows parallelization. This is not the case for other strategies such as (density gradient) ultracentrifugation,

which are often limited to six or eight samples and require expensive instrumentation. Size-exclusion chromatography (SEC) [42] requires sample concentration and is commonly set up in series, rather than in parallel. Moreover, SEC generally depends on Western blotting to identify those fractions that contain EV material and requires additional concentration steps. Commercial EV enrichment kits can be expensive and, more importantly, they show variability between suppliers [43, 44].

Here, we propose the use of 300 kDa MWCO filters for isolating and purifying EVs from conditioned cell medium (Figure 1), termed Filter-Aided Extracellular Vesicle Enrichment or FAEVEr. In brief, conditioned medium (CM) is isolated from cell culture and pre-cleared of loose cells, cell debris and large particles. Such pre-cleared CM is then transferred to a 300 kDa MWCO filter and the retentate is washed several times to remove abundant contaminating serum proteins and the cells' secretome. The filter-retained EVs are then lysed on the filter and the lysate is collected and processed for proteomics. We opted to directly lyse the filter-retained EVs in high (5%) concentrations of sodium dodecyl sulfate (SDS). The lysate is recovered by centrifugation and can be immediately processed for LC-MS/MS analysis using S-Trap columns [45] or used for Western blot applications. We show that the EV purity is highly improved when adding TWEEN-20 in relatively high concentrations and that low amounts of TWEEN-20 aid in the efficient recovery of EVs from the filter membrane without interfering with downstream nanoparticle tracking analysis (NTA). We explored differences in the EV protein cargo of cells incubated in medium containing different amounts of supplemented, EV-depleted fetal bovine serum (EVd FBS) as quite some discussion exists in the EV research field on the use of supplemented serum to cell cultures [46, 47] and its influence on EV content [48-50]. Some argue that serum is a potential source of EV contamination [46], whereas others reason that serum is essential to impede cell stress due to a lack of nutrients [51-53]. In fact, it was shown that cell starvation leads to drastic changes in the EV cargo [50], the number of released EVs [48] and their biogenesis [54]. Alternative biogenesis was found to be initiated by an upregulated autophagy pathway, thereby initiating the LC3-dependent EV loading and secretion

(LDELS) machinery [54]. Our obtained data links EV protein heterogeneity to an increased number of proteins involved in transcription, translation and cell cycle in EVs isolated from serum-deprived cell cultures. In addition, these EVs from serum deprived medium appear to be significantly devoid of (trans)membrane proteins.

D. Material and Methods

i. MCF7 cell culture and preclearing of conditioned medium

MCF7 cells of low passage number (< 10) were cultured using a standard protocol and equipment. MCF7 cells were seeded in T75 flasks with Dulbecco's Modified Eagle Medium (DMEM, Gibco) containing 10% standard FBS and incubated at 37 °C in 5% CO_2. When the cells reached 70-80% confluence, the medium was discarded and the cells were washed three times with PBS. Experiments were performed in duplicate, adding 8 mL of DMEM supplemented with either 0%, 2%, 5% or 10% EV-depleted FBS (EVd FBS, Thermo, A2720801). After 24 h, the conditioned media (CM) containing 0% EVd FBS was isolated, whereas the 2%, 5% and 10% EVd FBS containing CM were isolated after 48 h. The CM was immediately pre-cleared by two centrifugation rounds (500 x g for 5 min, and 10,000 x g for 10 min, room temperature) and filtration using 10 mL syringes equipped with 0.22 µm filters. The filtrate was collected and stored at -80 °C.

ii. Isolation of extracellular vesicles using 300 kDa MWCO filters and sample preparation

Moments before EV isolation, the CM was thawed and briefly vortexed. For each experiment, 3 mL of pre-cleared CM was used, diluted 1:1 with either PBS or 10% TWEEN-20 in PBS and vortexed vigorously for 10-15 s. The complete volume (6 mL) was loaded on a 300 kDa MWCO PES filter (Sartorius, Vivaspin®6, VS0652) and centrifuged (6,000 x g for 10-15 min at room temperature) using a Sorvall Lynx 4,000 centrifuge (Thermo) equipped with a F14x50cy rotor (Thermo, PN:096-145075). The filtrate was discarded and the retentate was washed using 1 mL wash buffer (PBS or 5% TWEEN-20 in PBS) and vortexed vigorously for 10-15 s before centrifugation (6,000 x g for 5-10 min at room temperature). After two rounds of washing, the retained particles were lysed on the filter using 100 µL 5% SDS in 50 mM TEAB, pH 7.4, and the EV lysates were collected by centrifugation (6,000 x g for 5 min at room temperature). The proteome was then prepared using S-Trap™ mini columns (ProtiFi, C02-mini-80) using the manufacturer's protocol. In brief, the proteins were reduced and alkylated using 5 mM TCEP (10 min at 55 °C) and 20 mM iodoacetamide (IAA, 10 min at room temperature in the dark), respectively, before acidifying the sample

to 1.2% phosphoric acid and diluting seven-fold with binding/wash buffer (90% methanol in 100 mM TEAB, pH 7.4). The samples were transferred to the corresponding S-Trap™ columns and each time centrifuged at 4,000 x g for 30 s during sample loading and washing. For protein digestion, 0.2 µg of trypsin (Promega, V5111) was added to 125 µL 50 mM TEAB (pH 7.4) and incubated overnight at 37 °C. The next day, the peptides were recovered by sequential elution by centrifugation (4,000 x g for 30 s at room temperature) using 80 µL 50 mM TEAB (pH 7.4), 80 µL 0.2% formic acid and 80 µL of 50% acetonitrile (ACN), 0.2% formic acid in dH_2O. The eluates (app. 365 µL) were transferred to MS vials, vacuum-dried in a SpeedVac and stored at -20 °C. Prior to LC-MS/MS analysis, samples were suspended in 30 µL of solvent A (2% ACN, 0.1% TFA in ddH_2O). We have submitted all relevant data of our experiments to the EV-TRACK knowledgebase (EV-TRACK ID: EV230600)[34].

iii. Cell harvest and sample preparation

Following isolation of the conditioned medium, the MCF7 cells were harvested. In short, the cells were washed three times with PBS before harvest using trypsin (Gibco, 25200056) for 5 min at 37 °C, 5% CO_2. The cells were pelleted (500 x g for 5 min), the pellet washed three times with PBS, solubilized in 100 µL PBS and transferred to a 96-well plate. After addition of 100 µL 2X lysis buffer (10% SDS in 100 mM TEAB, pH 7.4), the cells were sonicated (Pixul sonicator, pulse of 50 N, PRF of 1.0 kHz, burst rate of 20 Hz for 5 min) and the protein concentration was determined by a BCA assay. From each sample, a volume corresponding to 100 µg protein material was transferred to a fresh tube and diluted to 50 µL with 1X lysis buffer (final protein concentration of 2 µg/µL). The cellular proteomes were prepared using S-Trap™ mini columns (ProtiFi, C02-mini-80) using the manufacturer's protocol, as described in M&M section ii, using 1 µg of trypsin for digestion.

iv. HEK293T cell culture and production of recombinant EV material

A complete and detailed protocol for the transformation and production of recombinant EV (rEV) material is described in [55, 56]. In short, HEK293T cells of low passage number (< 10) were cultured using a standard cell culture protocol and equipment. Four million HEK293T cells were seeded in T75 flasks with DMEM containing 10% standard FBS and incubated for 48 h at 37 °C and in 5% CO_2. Then, the cells were transfected by adding a mixture of polyethyleneimine (PEI) and the DNA bait construct (12x, pMET7- GAG-eGFP) in 9.5 mL DMEM + 2% FBS for 6 h at 37 °C in 5% CO_2. The medium was then discarded and replaced with 8 mL fresh DMEM supplemented with 10% EVd FBS was added to the cells. After 48 h incubation at 37 °C in 5% CO_2, the cell transfection was evaluated under UV light (excitation at 488 nm and emission at 507 nm), the CM was isolated and immediately precleared as described in M&M section ii and frozen at -80 °C.

v. Western blot analysis of GAG-eGFP containing rEV particles

rEV particles were isolated from the CM and purified using the 300 kDa MWCO filtration protocol as described in M&M section ii, including 5% TWEEN-20 in PBS as washing buffer. From each centrifugation step, an aliquot was isolated for Western blot analysis. These aliquots were incubated for 5 min at 95 °C with XT sample buffer (4x) and XT reducing agent (20x) (BioRad). The protein material was separated by SDS-PAGE (4%-12%) for 80 min at 120 V prior to transfer onto a PVDF membrane (100 V, 30 min) and overnight incubation at 4 °C with primary antibodies (rabbit monoclonal anti-Calnexin (ab133615) and mouse monoclonal anti-HIV p24 39/5 4A (ab9071); 1:1,000). The next day, the membrane was incubated for 1 h at room temperature with secondary antibodies (goat anti-rabbit IRDye 680 CW and goat anti-mouse IRDye 800 CW; 1:10,000). Visualization was done on an Odyssey infrared imager (v3.0.16, LI-COR Biosciences).

vi. Recovery of EV particles from the 300 kDa MWCO membrane and Nanoparticle Tracking Analysis

100 µL of 0.1% TWEEN-20 in PBS was added to the filter after completing the EV enrichment protocol and shaken at 650 rpm for 5 min at room temperature. Then, the complete volume was transferred to a 2 mL tube and frozen. Immediately prior to nanoparticle analysis, the samples were thawed and diluted 10-fold in PBS before injecting 900 µL in the NTA instrument (ZetaView 8.04.02 SP2). The ZetaView settings were set to a temperature of 23 °C with an intensity and sensitivity of 70. The camera settings were set to 60 fps, 3 cycles and a frame rate of 30.

vii. LC-MS/MS analysis

Purified peptides from both EVs and MCF7 digested proteomes were re-dissolved in loading solvent A (0.1% TFA in water/ACN (98:2, v/v)) and the peptide concentration was determined on a Lunatic instrument (Unchained Lab). The samples were injected for LC-MS/MS analysis on an Ultimate 3000 RSLCnano system in-line connected to an Orbitrap Fusion Lumos mass spectrometer (Thermo). Trapping was performed at 20 µl/min for 2 min in loading solvent A on a Pepmap column (300 µm internal diameter (I.D.), 5 µm beads, C18, Thermo). The peptides were separated on a 110 cm µPAC prototype column (Thermo), kept at a constant temperature of 50 °C. Peptides were eluted by a non-linear gradient starting from 2% MS solvent B (0.1% formic acid (FA) in acetonitrile), reaching 26.4% MS solvent B in 82 min and 44% MS solvent B in 90 min and 56% MS solvent B in 100 min starting at a flowrate of 600 nl/min for 5 min, and completing the run at a flow rate of 300 nl/min, followed by a 5-minute wash at 56% MS solvent B and re-equilibration with MS solvent A (0.1% FA in water). The mass spectrometer was operated in data-independent mode. Full-scan MS spectra ranging from 390-900 m/z with a target value of 4E5, a maximum fill time of 50 ms and a resolution of 60,000 were followed by 50 quadrupole isolations with a precursor isolation width of 10 m/z for HCD fragmentation at an NCE of 34% after filling the trap at a target value of 4E5 for maximum injection time of 54 ms. MS2 spectra were acquired at a resolution of 30,000 at 200 m/z

in the Orbitrap analyser without multiplexing. The isolation intervals ranged from 400 – 900 m/z, without overlap. QCloud was used to control instrument longitudinal performance during the project [57, 58]. The mass spectrometry proteomics data have been deposited to the ProteomeXchange Consortium via the PRIDE [59] partner repository with the dataset identifier PXD043018.

viii. Database searching and analysis

Data-independent acquisition spectra were searched with the DIA-NN software (v1.8.1) [60] in library-free mode against the combination of two protein databases downloaded from Swiss-Prot; the complete human protein sequence database (January 2021, 20,394 sequences) supplemented with bovine serum protein sequences (March 2021, 618 sequences). The mass accuracy was set to 20 ppm and the MS1 accuracy to 10 ppm, with a precursor FDR of 0.01. Enzyme specificity was set to trypsin/P with a maximum of two missed cleavages. Variable modifications were set to oxidation of methionine residues (to sulfoxides) and acetylation of protein N-termini. Carbamidomethylation of cysteines was set as a fixed modification. The peptide length range was set to 7-30 residues with a precursor charge state between 1-4. The m/z range was set between 400-900 and 200-1,800 for the precursor and fragment ions, respectively. Cross-run normalization was set to RT dependent with the quantification strategy set to high accuracy and the neural network classifier to double-pass mode. The result file was further processed in KNIME (v4.3.3) by removing non-proteotypic peptides and identifications with a q-value above 0.01. Peptide quantifications were aggregated to protein group quantifications using the median of the corresponding normalized LFQ values. Further data analysis was performed with Perseus (version 1.6.14.0).

For the analysis of the EV and cellular proteomes across different experimental conditions, proteins that were significantly differentially abundant were identified by multiple sample testing (ANOVA, FDR < 0.05) and selected for hierarchical clustering (Euclidean distance with averaged linkage) after Z-scoring the

individual proteins over the different conditions. Row clusters were defined manually and used for gene ontology (GO) enrichment against the corresponding initial database (4,344 and 8,114 proteins for the EV and cellular analyses, respectively) and included biological process (GOBP), molecular function (GOMF), cellular component (GOCC) annotations and KEGG pathways. GO term enrichment was done using Fischer exact testing with an FDR threshold < 0.01 (Benjamin-Hochberg). Graphs and plots were made in GraphPad Prism (v9.4.1).

E. Results

FAEVEr workflow for enriching EVs from conditioned medium using 300 kDa MWCO filters

We reasoned that a simple filtration strategy may be a valid approach to isolate and purify EVs from the supernatant with our general outline of the FAEVEr workflow shown in Figure 1. In short, conditioned medium is isolated from cell cultures and pre-cleared by centrifugation (500 x g for 5 min and 10,000 x g for 10 min) and filtration (0.22 µm) to remove cell debris and large particles. The pre-cleared medium is subsequently loaded on filters and briefly centrifuged (10-15 min) at moderate speed (6,000 x g). We opted for 300 kDa MWCO polyether sulfone (PES) filters, which are hydrophilic and have low protein binding capacities. The filter membrane retains larger particles (including EVs) on the filter (the retentate), whereas smaller (non-EV) globular proteins are collected in the flow-through (the filtrate). The retentate is then washed several times with washing buffer to remove excess proteins and thereby improve the overall EV purity. The intact retentate can then either be recovered from the filter or immediately lysed by adding lysis buffer immediately on top of the filter, thereby releasing the EV proteome, hence enabling its efficient and quantitative recovery.

Despite the potential that ultrafiltration offers for the isolation of EVs from conditioned medium, several factors challenge its implementation. Most notably are the blockage of the filter membrane and the accompanying incomplete flow-through of the sample, the inefficient recuperation of intact EVs from the filter and the insufficient purity of retained EVs for proteome analysis. To avoid filter membranes getting clogged and improve sample flow-through, the sample viscosity was reduced by diluting the sample two-fold with PBS prior to loading and increasing the temperature during centrifugation from room temperature to 37 °C [61]. Implementing these factors reduced the centrifugation time considerably and induced consistent and uniform sample flow-through. After loading the sample, both EV and non-EV material are retained on the filter membrane, which then requires washing steps to improve the purity

by removing non-EV material. We initially opted to use phosphate buffered saline (PBS) as it has been widely used in other EV enrichment strategies as a diluent or washing buffer during ultracentrifugation [62], or as the mobile phase in size-exclusion chromatography [63]. For the recovery of the EV proteome, we decided that the most efficient recuperation would be a direct lysis of the filter-retained EVs, followed by collecting the EV cargo by centrifugation. To ensure complete lysis and recovery of protein material, high percentages of sodium dodecyl sulfate (SDS) were used, which is one of the most efficient detergents for membrane lysis, disrupting protein-protein interactions and (membrane) protein solubilization [64]. Note that SDS used to be irreconcilable with LC-MS/MS analysis [65, 66] however, the recently introduced suspension-trap columns (S-Trap) [45, 67] overcame this issue. In addition, the S-Trap protocol is fast, easy and reproducible, explaining why we opted for this protocol.

Low percentages of TWEEN-20 facilitate the recovery of EVs from 300 kDa MWCO filter membranes

The capability of efficiently recovering EV material from filter membranes is required to conduct quantitative and qualitative studies such as nanoparticle tracking analysis (NTA) and electron microscopy (EM) visualization. However, such quantitative recovery of EV material was reported to be troublesome on filters with a MWCO > 10 kDa [39]. To explore EV recovery from filters, we divided a rEV aliquot [56, 68] over eight individual fractions. Six fractions were filtered on 300 kDa MWCO filters, including three rounds of washing with PBS, and two fractions were kept in solution for use as standards. Following filtration, the retained rEV material was recovered by adding 1 mL PBS with either 0%, 0.1% or 1% TWEEN-20 [41] combined with vigorous vortexing. The rEV material was isolated, diluted with the corresponding buffer and analyzed by NTA. In line with the findings of Vergauwen *et al*. [39], we found that recovery of rEV material using PBS is inefficient. However, addition of TWEEN-20 to PBS greatly improved rEV recovery to nearly the same numbers of particles observed in the standards (rEV fraction in solution) (**Figure 2A**) with the same size distribution (Figure 2B). Here, it must be noted that with an increasing percentage of

TWEEN-20, we also observed an increased scattering intensity, likely due to the formation of air bubbles during NTA injection with a syringe, thereby skewing the results. This was observed during the measurements of rEVs recovered in 1% TWEEN-20. Our results indicate that 0.1% TWEEN-20 in PBS efficiently recovers rEV material from the filter membrane and that NTA measurements are unaffected at this TWEEN-20 concentration.

TWEEN-20 aids in the removal of non-EV proteins during EV enrichment on 300 kDa MWCO filters

To further improve EV purification on 300 kDa MWCO filters, we explored mild detergents to improve solubility and minimize protein-membrane interactions. EVs, being delineated by a lipid bilayer, are susceptible to detergent-mediated lysis. Osteikoetxea and co-workers have explored the minimum required concentration of detergents for efficient lysis of EV particles in solution [69]. Next to describing such concentrations for different detergents, they also show that these concentrations varied between EV subpopulations (exosomes, microvesicles and apoptotic bodies). Especially the smallest (exosomal) subpopulation was found to show a decreased susceptibility against detergents compared to larger vesicles (microvesicles and apoptotic bodies), as summarized in **Table 1**, due to their increased liquid order compared to larger vesicles [70, 71] as a consequence of an accumulation of cholesterol and sphingolipids during their formation [72].

Table 1: Summary of the concentrations of different detergents inducing lysis per EV subpopulation. Data taken from Osteikoetxa et al. (2015).

	SDS (W:V)	TRITON X-100 (V:V)	DEOXYCHOLATE (W:V)	TWEEN-20 (V:V)
APOPTOTIC BODIES	0.005 - 0.010%	0.010 - 0.025%	0.025 - 0.050%	5.0 - 10.0%
MICROVESICLES	0.005 - 0.010%	0.010 - 0.025%	0.025 - 0.050%	5.0 - 10.0%
EXOSOMES	0.075 - 0.125%	0.050 - 0.075%	0.075 - 0.100%	10.0 - 15.0%

Table 1 indicates that EVs have a high tolerance against the mild detergent TWEEN-20, which is often used in other biochemical assays (e.g. Western blot) to reduce non-specific protein adherence to membranes [73]. Contrary to SDS, which appears to already lyse the bulk of EV material in solution at low percentages (0.025%) (Supplementary Figure 1). Therefore, TWEEN-20 was here explored to improve the washing steps during 300 kDa MWCO filtration.

First, we validated that supplementing TWEEN-20 to the wash buffer removed contaminating non-EV proteins. Therefore, pre-cleared conditioned medium from MCF7 cells was filtered on a 300 kDa MWCO filter and washed with PBS with or without different percentages of TWEEN-20. The individual flow-through fractions from both the wash and lysis steps were collected, loaded on SDS-PAGE and stained with Coomassie (**Supplementary Figure 2**). Comparing the band intensities around 65 kDa (albumin) of the wash fractions between the different conditions revealed that PBS without TWEEN-20 was the least capable at removing the bulk of serum protein material. This is in contrast to the lysate fractions, where the 65 kDa band remains clearly visible in the PBS lane, but is absent when TWEEN-20 is supplemented to the wash buffer.

Secondly, we confirmed that high concentrations of TWEEN-20 had no detrimental effect on the EV integrity, which was demonstrated on CM of HEK293T cells transfected with a GAG-eGFP construct to produce GAG HIV-1 virus-like particles, further referred to as recombinant EVs (rEVs) [56, 68]. The pre-cleared CM containing a final concentration of 5% TWEEN-20 was loaded on the filter and centrifuged. The retentate was subsequently washed several times with a buffer containing 5% TWEEN-20. Per centrifugation round, the flow-through was used for Western blot analysis (). No GAG-eGFP signal was observed in the flow-through after sample loading or washing, indicating that the rEV particles are retained on the filter and not lysed when applying 5% TWEEN-20, in line with earlier findings [69]. In

addition, an intense signal was observed in the flow-through from the lysate (in 5% SDS) fraction, indicating that EV proteins are efficiently recovered.

Serum depletion during cell culture drastically affects the proteome of MCF7 cells and its EVs

Upon analyzing publicly available EV-TRACK data, we found that of the 1,160 EV-TRACK experiments submitted during the past 5 years (2018-2022), 53% of human cell culture experiments were conducted in EV-depleted serum, whereas 36% chose not to add serum (Figure 4). To investigate the effects of serum deprivation on the EV cargo, we cultured MCF7 cells in DMEM containing either 0%, 2%, 5% or 10% EVd FBS (D0, D2, D5 and D10, respectively). During cell culture, the CM of D0 was harvested after 24 h as beyond this point cell death increases rapidly [74]. In contrast, the CM of cells grown in EVd FBS (D2, D5 and D10) were collected after 48 h [75, 76].

In addition, we also investigated the cellular proteomes of the corresponding EV-producing MCF7 cells grown in DMEM supplemented with different percentages of EVd FBS, as well as DMEM supplemented with 10% standard (non EV-depleted) FBS (**Supplementary data 1)**. The latter was included as we noticed that the protein concentration of EVd FBS is about six times lower than that of standard FBS (Supplementary Figure 3**A**), which is due to the fact that prior to the depletion of EVs from FBS, FBS is diluted several times (up to five times) to avoid protein aggregation and subsequent pelleting during ultracentrifugation due to its high viscosity [77]. To verify that EVd FBS has no detrimental effect on the MCF7 cells in culture, we first compared the cellular proteome of MCF7 cells cultured in 10% EVd FBS or 10% standard FBS. We identified 8,114 proteins in total (Supplementary Figure 3**B)**, of which 7,579 were included for quantitative analysis after disposing of proteins with less than two valid values in at least one group and missing values were imputed. Thirteen proteins (0.17%) were found to be significantly differentially expressed ($\log_2$ difference > |1| and $-\log_{10}$(p-value) > 2), of which three were more abundant in the 10% FBS condition and 10 more abundant in the 10% EVd FBS condition (Supplementary Figure 3**C)**.

We did not observe any specific enrichment in gene ontology molecular function (GOMF), biological process (GOBP) nor cellular component (GOCC), and therefore concluded that switching from 10% standard FBS to 10% EVd FBS has no major impact on the proteome of MCF7 cells.

To investigate if our approach removed the bulk of non-EV proteins from the conditioned medium during EV enrichment on 300 kDa MWCO filters, we compared the EV proteomes after washes with either PBS or PBS supplemented with 5% TWEEN-20. When using only PBS, approximately 3.6% of the identified proteins were of bovine origin in the D0 condition (residual bovine proteins), but this fraction went up to 12.1% in the D10 condition (Figure 5**A**). This fraction of contaminating proteins was reduced, albeit moderately, in the TWEEN-20 wash steps to 7.1% in the D10 condition. However, more informative is the relative share of the spectral space or intensity that was occupied by bovine peptide precursor ions compared to the total intensity of the ion chromatogram (TIC). We observed that bovine peptide ions accounted for 6.8% to nearly 30% of TIC at D0 and D10, respectively. However, upon introducing 5% TWEEN-20 to the washing buffer, we observed a decrease in bovine TIC contaminations to 16.9% for D10 at the precursor intensity level (Figure 5**B**).

Comparing the total number of protein identifications with the number of protein identifications in the D0 condition revealed drastic differences between the EV proteomes (**Supplementary data 2**). Across the different experiments using 5% TWEEN-20 as washing buffer, over 4,344 human proteins were identified in total, from which 3,469 (76%) were identified with two valid values in at least one experiment and 1,027 were found in each experiment (n = 8) (**Figure 5C**). A closer look revealed that of these 3,469 proteins, 1,004 proteins (29%) were uniquely found in D0. After enrichment and purification of the EVs on the 300 kDa MWCO membrane, a small fraction was recovered from each replicate and pooled per experimental condition for NTA analysis. We observed a normal size distribution that slightly increased from approximately 145 nm to 176 nm for D0 and D10, respectively. In addition, we observed that D0 contained

approximately double the number of particles compared to D2, D5 and D10 (Figure 5**D**). Next, we mapped six well-known molecular protein markers for EVs (CD9, CD63, CD81, SDCBP, PDCD6IP (Alix) and TSG101), which were found across all proteomic experiments (Figure 5**E)**, again indicating that EVs were not only successfully retained and purified, but also that we are able to efficiently recover the EV protein cargo and transmembrane proteins by immediately lysing EVs on the filter with high concentrations of SDS.

To allow comparison between the conditions, we removed the 1,004 unique proteins in D0 from the statistical analysis. From the remaining 2,099 proteins, 654 were significantly more abundant following multiple-sample testing (ANOVA, permutation-based FDR < 0.05). Hierarchical clustering of these proteins with z-scored intensities revealed two major clusters between the EV proteomes from serum depleted (D0) and serum supplemented (D2-D5-D10) medium, containing 337 and 317 proteins, respectively (**Figure 6A**). Before the GO enrichment, we combined the proteins that were significantly more abundant in D0 together with the 1,004 unique proteins that were removed prior to the statistical analysis. The GO enrichment of the two clusters resulted in 140 and 135 GO terms that were significantly enriched or deprived for the serum depleted and serum containing conditions, respectively. Strikingly, we observed a major contrast between the two populations as proteins that were significantly more abundant in the serum depleted conditions were highly associated with biosynthetic functions (e.g. cell cycle and transcription/translation) and metabolism (Figure 6**B**), yet significantly devoid of transmembrane (TM) proteins (**Figure 6C**). This was the opposite in the serum containing conditions, were TM proteins and TM-associated functions (TM transport, adhesion and receptor/signaling) where highly abundant as well as terms associated with proliferation and exo/endocytosis (**Figure 6C**). However, fewer proteins associated with biosynthetic functions and metabolism were found.

A closer investigation of the proteomes of the parental cells revealed additional intriguing insights (**Supplementary data 1**). After selecting the ANOVA significant hits and hierarchical clustering

(Supplementary Figure 4), we again observed two clusters (albeit not as distinct as in its EV counterpart) containing 516 proteins that were more abundantly expressed in the serum containing conditions and 336 proteins in the serum depleted conditions. GO analysis of these clusters revealed that the proteome isolated from cells grown in serum depleted medium is specifically enriched in diverse metabolic salvation pathways using alternative carbon sources (e.g. aldehyde and ketone metabolic processes). Whereas the proteomes of cells isolated from serum containing medium have a higher abundance of proteins associated with biosynthetic processes such as translation and cell cycle (**Figure 6B**).

In addition to the GO analysis of the EVs, we further investigated the presence of autophagy related proteins (ATGs), as it was previously shown that ATGs are important effectors of EV secretion [78]. For instance, the ATG5-ATG16L1 complex is associated with the dissociation of V-ATPase, which prevents the acidification of MVBs and therefore the lysosomal degradation, hence promoting the MVB fusion with the PM [79]. We observed that several of the main ATG proteins and contributors to phagosome biogenesis are highly abundant in the EVs isolated from serum depleted conditions and absent in serum-containing conditions (Figure 6**D**). This might indicate that during starvation-induced autophagy, lysosomal activity is insufficient and alternative pathways are activated for the secretion of unwanted biomaterial [80].

F. Discussion

Despite the potential of extracellular vesicles (EVs) towards clinical applications as circulating biomarkers and as therapeutic shuttles, their efficient isolation and purification in a cost-effective manner remains a major bottleneck. Here, we proposed a 300 kDa MWCO filtration strategy for the enrichment of EVs from conditioned medium. Our data shows that EVs are successfully retained on the filter and that the bulk of unwanted, non-EV proteins are removed using wash buffers that contain relative high percentages of TWEEN-20. As a proof-of-concept we used recombinant EV particles derived from GAG-eGFP transfected HEK293T cells [68]. Our data shows that such particles, present in complex medium containing 10% EV depleted FBS (EVd FBS), are retained on the filter membrane and remain intact when applying washing buffer containing 5% TWEEN-20. In addition, we demonstrate that the retained particles can be successfully recovered from the filter membrane using trace amounts of TWEEN-20 in a re-suspension buffer, with no effect on NTA particle analysis.

We applied our strategy to isolate and purify EVs from conditioned medium of MCF7 cells grown in DMEM medium containing different percentages of EVd FBS (0%, 2%, 5% and 10%). Proteome analysis of the EV lysates indicated a large difference in proteome between EVs isolated from serum-depleted versus serum-containing medium. In summary, our data indicates that starvation of MCF7 cells initiates not only stress on the cell itself, but that the implications of cellular starvation are also observed in the EV protein cargo. In line with Leidal *et al*. [81], we observed a significant increase in RNA-binding proteins in the proteome of EVs stemming from cells grown in serum-depleted medium. More specifically, during serum depletion, EVs are packed with proteins that are associated with anabolic processes or biogenesis of cell material such as translation and transcription regulation. This is somewhat counterintuitive, as starvation leads to disposal of valuable EV packed building blocks that, alternatively, could be recycled via lysosomal degradation. This also suggests that during cell starvation, cell survival is sustained by stimulating the core metabolic processes whilst inhibiting cell proliferation by disposing of the major constituents of protein

synthesis and the cell cycle to obtain some sort of hard stop. This is in contrast to the proteomes of EVs recovered from cells grown in serum-containing medium, in which much more transmembrane proteins were observed. We conclude that deprivation of serum during cell culture has a significant effect on the EV cargo and that transmembrane proteins are possibly underrepresented due to their rapid degradation [82, 83]. Therefore, if not properly considered beforehand, undisclosed effects of the serum deprivation might bias the preconceived working hypothesis as it might lead to misinterpretation of the (proteomics) data and hamper experimental reproducibility [51].

During the development of the ultrafiltration approach, we limited the input to 3 mL of conditioned medium, approximately a third of the conditioned medium typically isolated from one T75 cell culture flask per replicate, facilitating cell culture and general sample handling. This is in contrast to several other approaches (e.g. ultracentrifugation, density gradient ultracentrifugation and size-exclusion chromatography) where starting volumes of more than 10 mL are not uncommon. However, such higher volumes often require sample concentration steps prior to EV isolation by e.g. density gradient ultracentrifugation and size exclusion chromatography, thereby potentially contributing to unnecessary variability.

Although this study was limited to 300 kDa MWCO filter devices with 6 mL volume capacity and we used 3 mL of conditioned medium, other spin columns are available with varying loading capacities, both larger (e.g. 20 mL capacity in a 50 mL falcon format) and smaller (500 µL capacity in a 1.5 mL tube format). The latter allows for parallelization of 24 samples using conventional bench-top centrifuges. In addition, 96-well plate formats are available, ranging between 300 and 400 µL loading capacity. Translating the strategy to a 96-well plate format in particular would allow to efficiently analyze EVs isolated from different conditions, cell lines and treatments, whilst minimizing batch-to-batch variability. Furthermore, while not shown here, our filtration-based strategy potentially offers additional applications besides

proteome analysis. For instance, our strategy could be modified towards RNA screening as oligonucleotides (including lncRNA [84], miRNA [85] and mRNA [86]) have become a major topic of research in the EV field.

In conclusion, we showed that the 300 kDa MWCO filtration strategy is effective for the enrichment of EVs from conditioned medium. Our approach is capable of retaining EVs on the filter and maintaining their intactness whilst removing undesired components using buffers containing mild detergents. In addition, we have shown the capability of our method to recover intact, purified EVs from the filter for NTA purposes or to immediately recover the EV proteome cargo following lysis. Our proteomics data confirms that the filtration strategy is capable of delivering purity levels suitable for downstream analysis by mass spectrometry.

G. References

1. van Niel, G., G. D'Angelo, and G. Raposo, *Shedding light on the cell biology of extracellular vesicles.* Nature Reviews Molecular Cell Biology, 2018. **19**: p. 213.

2. Wei, D., et al., *RAB31 marks and controls an ESCRT-independent exosome pathway.* Cell Research, 2021. **31**(2): p. 157-177.

3. Mathieu, M., et al., *Specificities of secretion and uptake of exosomes and other extracellular vesicles for cell-to-cell communication.* Nature Cell Biology, 2019. **21**(1): p. 9-17.

4. Elmore, S., *Apoptosis: a review of programmed cell death.* Toxicol Pathol, 2007. **35**(4): p. 495-516.

5. Arteaga-Blanco, L.A., et al., *Characterization and internalization of small extracellular vesicles released by human primary macrophages derived from circulating monocytes.* PLOS ONE, 2020. **15**(8): p. e0237795.

6. Wang, Y., et al., *Apoptotic cell-derived micro/nanosized extracellular vesicles in tissue regeneration.* 2022. **11**(1): p. 957-972.

7. Cocucci, E. and J. Meldolesi, *Ectosomes and exosomes: shedding the confusion between extracellular vesicles.* Trends in Cell Biology, 2015. **25**(6): p. 364-372.

8. Hoshino, A., et al., *Tumour exosome integrins determine organotropic metastasis.* Nature, 2015. **527**(7578): p. 329-35.

9. French, K.C., M.A. Antonyak, and R.A. Cerione, *Extracellular vesicle docking at the cellular port: Extracellular vesicle binding and uptake.* Seminars in cell & developmental biology, 2017. **67**: p. 48-55.

10. Ludwig, A.-K. and B. Giebel, *Exosomes: Small vesicles participating in intercellular communication.* The International Journal of Biochemistry & Cell Biology, 2012. **44**(1): p. 11-15.

11. Takahashi, A., et al., *Exosomes maintain cellular homeostasis by excreting harmful DNA from cells.* Nature Communications, 2017. **8**(1): p. 15287.

12. Hamzah, R.N., et al., *Exosome Traceability and Cell Source Dependence on Composition and Cell-Cell Cross Talk.* Int J Mol Sci, 2021. **22**(10).

13. Dong, Q., et al., *Pre-metastatic Niche Formation in Different Organs Induced by Tumor Extracellular Vesicles.* Front Cell Dev Biol, 2021. **9**: p. 733627.

14. Zhang, W., et al., *Engineered Cancer-Derived Small Extracellular Vesicle-Liposome Hybrid Delivery System for Targeted Treatment of Breast Cancer.* ACS Appl Mater Interfaces, 2023.

15. Hoffmann, O., et al., *Programmed death receptor ligand-2 (PD-L2) bearing extracellular vesicles as a new biomarker to identify early triple-negative breast cancer patients at high risk for relapse.* J Cancer Res Clin Oncol, 2022.

16. K, S., D. T, and P. M, *Small extracellular vesicles as a multicomponent biomarker platform in urinary tract carcinomas.* Frontiers in Molecular Biosciences, 2022. **9**.

17. Gao, X., B. Gao, and S. Li, *Extracellular vesicles: A new diagnostic biomarker and targeted drug in osteosarcoma.* Front Immunol, 2022. **13**: p. 1002742.

18. Vandendriessche, C., D. Kapogiannis, and R.E. Vandenbroucke, *Biomarker and therapeutic potential of peripheral extracellular vesicles in Alzheimer?s disease.* Advanced Drug Delivery Reviews, 2022. **190**.

19. Newman, L.A., K. Muller, and A. Rowland, *Circulating cell-specific extracellular vesicles as biomarkers for the diagnosis and monitoring of chronic liver diseases.* Cellular and Molecular Life Sciences, 2022. **79**(5): p. 232.

20. Welton, J.L., et al., *Cerebrospinal fluid extracellular vesicle enrichment for protein biomarker discovery in neurological disease; multiple sclerosis.* Journal of Extracellular Vesicles, 2017. **6**(1).

21. Horvatovich, P.L. and R. Bischoff, *Current Technological Challenges in Biomarker Discovery and Validation.* European Journal of Mass Spectrometry, 2010. **16**(1): p. 101-121.

22. Stam, J., et al., *Isolation of extracellular vesicles with combined enrichment methods.* Journal of Chromatography B, 2021. **1169**: p. 122604.

23. Vanderboom, P.M., et al., *A size-exclusion-based approach for purifying extracellular vesicles from human plasma.* Cell Reports Methods, 2021. **1**(3): p. 100055.

24. Onódi, Z., et al., *Isolation of High-Purity Extracellular Vesicles by the Combination of Iodixanol Density Gradient Ultracentrifugation and Bind-Elute Chromatography From Blood Plasma.* Frontiers in physiology, 2018. **9**: p. 1479-1479.

25. Gallart-Palau, X., et al., *Extracellular vesicles are rapidly purified from human plasma by PRotein Organic Solvent PRecipitation (PROSPR).* Scientific Reports, 2015. **5**(1): p. 14664.

26. Rider, M.A., S.N. Hurwitz, and D.G. Meckes, *ExtraPEG: A Polyethylene Glycol-Based Method for Enrichment of Extracellular Vesicles.* Scientific Reports, 2016. **6**(1): p. 23978.

27. Brambilla, D., et al., *EV Separation: Release of Intact Extracellular Vesicles Immunocaptured on Magnetic Particles.* Anal Chem, 2021.

28. Vergauwen, G., et al., *Robust sequential biophysical fractionation of blood plasma to study variations in the biomolecular landscape of systemically circulating extracellular vesicles across clinical conditions.* J Extracell Vesicles, 2021. **10**(10): p. e12122.

29. Tian, F., et al., *Protein analysis of extracellular vesicles to monitor and predict therapeutic response in metastatic breast cancer.* Nat Commun, 2021. **12**(1): p. 2536.

30. Askeland, A., et al., *Mass-Spectrometry Based Proteome Comparison of Extracellular Vesicle Isolation Methods: Comparison of ME-kit, Size-Exclusion Chromatography, and High-Speed Centrifugation.* Biomedicines, 2020. **8**(8).

31. An, M., et al., *Comparison of an Optimized Ultracentrifugation Method versus Size-Exclusion Chromatography for Isolation of Exosomes from Human Serum.* J Proteome Res, 2018. **17**(10): p. 3599-3605.

32. Brennan, K., et al., *A comparison of methods for the isolation and separation of extracellular vesicles from protein and lipid particles in human serum.* Scientific Reports, 2020. **10**(1): p. 1039.

33. Baranyai, T., et al., *Isolation of Exosomes from Blood Plasma: Qualitative and Quantitative Comparison of Ultracentrifugation and Size Exclusion Chromatography Methods.* PLOS ONE, 2015. **10**(12): p. e0145686.

34. Van Deun, J., et al., *EV-TRACK: transparent reporting and centralizing knowledge in extracellular vesicle research.* Nature Methods, 2017. **14**(3): p. 228-232.

35. Théry, C., et al., *Minimal information for studies of extracellular vesicles 2018 (MISEV2018): a position statement of the International Society for Extracellular Vesicles and update of the MISEV2014 guidelines.* Journal of Extracellular Vesicles, 2018. **7**(1): p. 1535750.

36. Lobb, R.J., et al., *Optimized exosome isolation protocol for cell culture supernatant and human plasma.* Journal of extracellular vesicles, 2015. **4**: p. 27031-27031.

37. Guan, S., et al., *Characterization of Urinary Exosomes Purified with Size Exclusion Chromatography and Ultracentrifugation.* Journal of Proteome Research, 2020. **19**(6): p. 2217-2225.

38. Gámez-Valero, A., et al., *Size-Exclusion Chromatography-based isolation minimally alters Extracellular Vesicles' characteristics compared to precipitating agents.* Scientific Reports, 2016. **6**(1): p. 33641.

39. Vergauwen, G., et al., *Confounding factors of ultrafiltration and protein analysis in extracellular vesicle research.* Sci Rep, 2017. **7**(1): p. 2704.

40. Jordan, K.R., et al., *Extracellular vesicles from young women's breast cancer patients drive increased invasion of non-malignant cells via the Focal Adhesion Kinase pathway: a proteomic approach.* Breast Cancer Research, 2020. **22**(1): p. 128.

41. Allelein, S., et al., *Potential and challenges of specifically isolating extracellular vesicles from heterogeneous populations.* Sci Rep, 2021. **11**(1): p. 11585.

42. Sidhom, K., P.O. Obi, and A. Saleem, *A Review of Exosomal Isolation Methods: Is Size Exclusion Chromatography the Best Option?* Int J Mol Sci, 2020. **21**(18).

43. Ding, M., et al., *Comparison of commercial exosome isolation kits for circulating exosomal microRNA profiling.* Analytical and Bioanalytical Chemistry, 2018. **410**(16): p. 3805-3814.

44. Royo, F., et al., *Different EV enrichment methods suitable for clinical settings yield different subpopulations of urinary extracellular vesicles from human samples.* Journal of Extracellular Vesicles, 2016. **5**(1): p. 29497.

45. HaileMariam, M., et al., *S-Trap, an Ultrafast Sample-Preparation Approach for Shotgun Proteomics.* Journal of Proteome Research, 2018. **17**(9): p. 2917-2924.

46. Lehrich, B.M., Y. Liang, and M.S. Fiandaca, *Foetal bovine serum influence on in vitro extracellular vesicle analyses.* Journal of extracellular vesicles, 2021. **10**(3): p. e12061-e12061.

47. Lehrich, B.M., et al., *Fetal Bovine Serum-Derived Extracellular Vesicles Persist within Vesicle-Depleted Culture Media.* International Journal of Molecular Sciences, 2018. **19**(11).

48. Sun, L., et al., *Serum deprivation elevates the levels of microvesicles with different size distributions and selectively enriched proteins in human myeloma cells in vitro.* Acta Pharmacologica Sinica, 2014. **35**(3): p. 381-393.

49. Kakarla, R., et al., *Apoptotic cell-derived exosomes: messages from dying cells.* Experimental & Molecular Medicine, 2020. **52**(1): p. 1-6.

50. Li, J., et al., *Serum-free culture alters the quantity and protein composition of neuroblastoma-derived extracellular vesicles.* J Extracell Vesicles, 2015. **4**: p. 26883.

51. Rashid, M.-u. and K.M. Coombs, *Serum-reduced media impacts on cell viability and protein expression in human lung epithelial cells.* Journal of Cellular Physiology, 2019. **234**(6): p. 7718-7724.

52. Shin, J., et al., *Comparative analysis of differentially secreted proteins in serum-free and serum-containing media by using BONCAT and pulsed SILAC.* Scientific Reports, 2019. **9**(1): p. 3096.

53. He, L., et al., *Autophagy: The Last Defense against Cellular Nutritional Stress.* Advances in Nutrition, 2018. **9**(4): p. 493-504.

54. Leidal, A.M., et al., *The LC3-conjugation machinery specifies the loading of RNA-binding proteins into extracellular vesicles.* Nature Cell Biology, 2020. **22**(2): p. 187-199.

55. Eyckerman, S., et al., *Trapping mammalian protein complexes in viral particles.* Nature Communications, 2016. **7**(1): p. 11416.

56. Geeurickx, E., et al., *The generation and use of recombinant extracellular vesicles as biological reference material.* Nature Communications, 2019. **10**(1): p. 3288.

57. Olivella, R., et al., *QCloud2: An Improved Cloud-based Quality-Control System for Mass-Spectrometry-based Proteomics Laboratories.* Journal of Proteome Research, 2021. **20**(4): p. 2010-2013.

58. Chiva, C., et al., *QCloud: A cloud-based quality control system for mass spectrometry-based proteomics laboratories.* PLOS ONE, 2018. **13**(1): p. e0189209.

59. Perez-Riverol, Y., et al., *The PRIDE database resources in 2022: a hub for mass spectrometry-based proteomics evidences.* Nucleic Acids Res, 2022. **50**(D1): p. D543-d552.

60. Demichev, V., et al., *DIA-NN: neural networks and interference correction enable deep proteome coverage in high throughput.* Nat Methods, 2020. **17**(1): p. 41-44.

61. Çinar, Y., A.M. Şenyol, and K. Duman, *Blood viscosity and blood pressure: role of temperature and hyperglycemia.* American Journal of Hypertension, 2001. **14**(5): p. 433-438.

62. Amor López, A., et al. *Inactivation of EMILIN-1 by Proteolysis and Secretion in Small Extracellular Vesicles Favors Melanoma Progression and Metastasis*. International Journal of Molecular Sciences, 2021. **22**, DOI: 10.3390/ijms22147406.

63. Coughlan, C., et al., *Exosome Isolation by Ultracentrifugation and Precipitation and Techniques for Downstream Analyses.* Current Protocols in Cell Biology, 2020. **88**(1): p. e110.

64. Elinger, D., A. Gabashvili, and Y. Levin, *Suspension Trapping (S-Trap) Is Compatible with Typical Protein Extraction Buffers and Detergents for Bottom-Up Proteomics.* Journal of Proteome Research, 2019. **18**(3): p. 1441-1445.

65. Varnavides, G., et al., *In Search of a Universal Method: A Comparative Survey of Bottom-Up Proteomics Sample Preparation Methods.* Journal of Proteome Research, 2022. **21**(10): p. 2397-2411.

66. Ludwig, K.R., M.M. Schroll, and A.B. Hummon, *Comparison of In-Solution, FASP, and S-Trap Based Digestion Methods for Bottom-Up Proteomic Studies.* J Proteome Res, 2018. **17**(7): p. 2480-2490.

67. Chhuon, C., et al., *A sensitive S-Trap-based approach to the analysis of T cell lipid raft proteome.* J Lipid Res, 2020. **61**(11): p. 1512-1523.

68. Geeurickx, E., et al., *Recombinant extracellular vesicles as biological reference material for method development, data normalization and assessment of (pre-)analytical variables.* Nat Protoc, 2021.

69. Osteikoetxea, X., et al., *Differential detergent sensitivity of extracellular vesicle subpopulations.* Organic & Biomolecular Chemistry, 2015. **13**(38): p. 9775-9782.

70. Osteikoetxea, X., et al., *Improved Characterization of EV Preparations Based on Protein to Lipid Ratio and Lipid Properties.* PLOS ONE, 2015. **10**(3): p. e0121184.

71. Choi, D.S., et al., *Proteomics, transcriptomics and lipidomics of exosomes and ectosomes.* Proteomics, 2013. **13**(10-11): p. 1554-71.

72. Subra, C., et al., *Exosome lipidomics unravels lipid sorting at the level of multivesicular bodies.* Biochimie, 2007. **89**(2): p. 205-212.

73. Feng, M., et al., *Effects of Tween 20 on the desorption of proteins from polymer surfaces.* J Biomater Sci Polym Ed, 1995. **7**(5): p. 415-24.

74. Braun, F., et al., *Serum-nutrient starvation induces cell death mediated by Bax and Puma that is counteracted by p21 and unmasked by Bcl-x(L) inhibition.* PLoS One, 2011. **6**(8): p. e23577.

75. Rontogianni, S., et al., *Proteomic profiling of extracellular vesicles allows for human breast cancer subtyping.* Communications Biology, 2019. **2**(1): p. 325.

76. Salem, I., et al., *Methods for extracellular vesicle isolation from cancer cells.* Cancer Drug Resist, 2020. **3**(3): p. 371-384.

77. Théry, C., et al., *Isolation and characterization of exosomes from cell culture supernatants and biological fluids.* Curr Protoc Cell Biol, 2006. **Chapter 3**: p. Unit 3.22.

78. Leidal, A.M. and J. Debnath, *Emerging roles for the autophagy machinery in extracellular vesicle biogenesis and secretion.* FASEB Bioadv, 2021. **3**(5): p. 377-386.

79. Guo, H., et al., *Atg5 Disassociates the V1V0-ATPase to Promote Exosome Production and Tumor Metastasis Independent of Canonical Macroautophagy.* Developmental Cell, 2017. **43**(6): p. 716-730.e7.

80. Debnath, J., N. Gammoh, and K.M. Ryan, *Autophagy and autophagy-related pathways in cancer.* Nature Reviews Molecular Cell Biology, 2023.

81. Leidal, A.M. and J. Debnath, *Unraveling the mechanisms that specify molecules for secretion in extracellular vesicles.* Methods, 2020. **177**: p. 15-26.

82. Müller, M., et al., *The coordinated action of the MVB pathway and autophagy ensures cell survival during starvation.* eLife, 2015. **4**: p. e07736.

83. Jones, C.B., et al., *Regulation of membrane protein degradation by starvation-response pathways.* Traffic (Copenhagen, Denmark), 2012. **13**(3): p. 468-482.

84. Lv, S., J. Wang, and L. Li, *Extracellular vesicular lncRNA FAL1 promotes hepatocellular carcinoma cell proliferation and invasion by inducing macrophage M2 polarization.* J Physiol Biochem, 2023.

85. Niitsu, Y., et al., *Increased serum extracellular vesicle miR-144-3p and miR-486a-3p in a mouse model of adipose tissue regeneration promote hepatocyte proliferation by targeting Txnip.* PLoS One, 2023. **18**(5): p. e0284989.

86. Lázaro-Ibáñez, E., et al., *Distinct prostate cancer-related mRNA cargo in extracellular vesicle subsets from prostate cell lines.* BMC Cancer, 2017. **17**(1): p. 92.

H. Acknowledgements

The authors thank all operators of the VIB Proteomics Core facility for their excellence and input. The authors thenk the lab of An Hendrix for kindly providing us with the required purified rEV aliquots.

I. Data availability

The mass spectrometry proteomics data have been deposited to the ProteomeXchange Consortium via the PRIDE partner repository with the dataset identifier PXD043018.

J. Author contributions

JP planned, designed and performed the experiments and wrote the manuscript. JVDV assisted with experiments. TVDS performed the HEK293T cell culture and production of rEV material. All authors read and approved the manuscript.

K. Funding statement

K.G. and S.E. acknowledge support by a Strategic Basic Research project (EV-TRACE) from the Research Foundation -Flanders (FWO), project number S006319N.

L. Conflict of interest

The authors declare no conflict of interest.

M. Figures

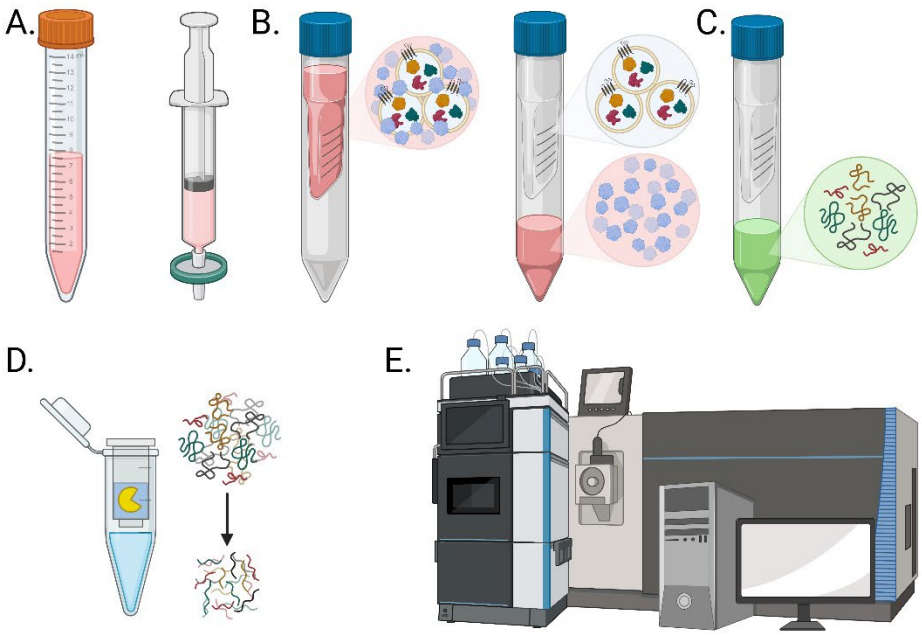

Figure 1: Schematic overview of the FAEVEr workflow. Conditioned medium is isolated from cell culture and pre-cleared (A) prior to loading the material on the 300 kDa MWCO filter. During centrifugation, the EV particles are retained on the filter (B), whereas unwanted protein material (e.g. serum proteins) is removed by washing the retentate with TWEEN-20 to further improve the purity of the EV sample. The EV cargo is efficiently recovered by immediately lysing the EVs on the filter (C) and processing the EV proteome using S-Trap columns (D) for LC-MS/MS analysis (E). Created with Biorender.

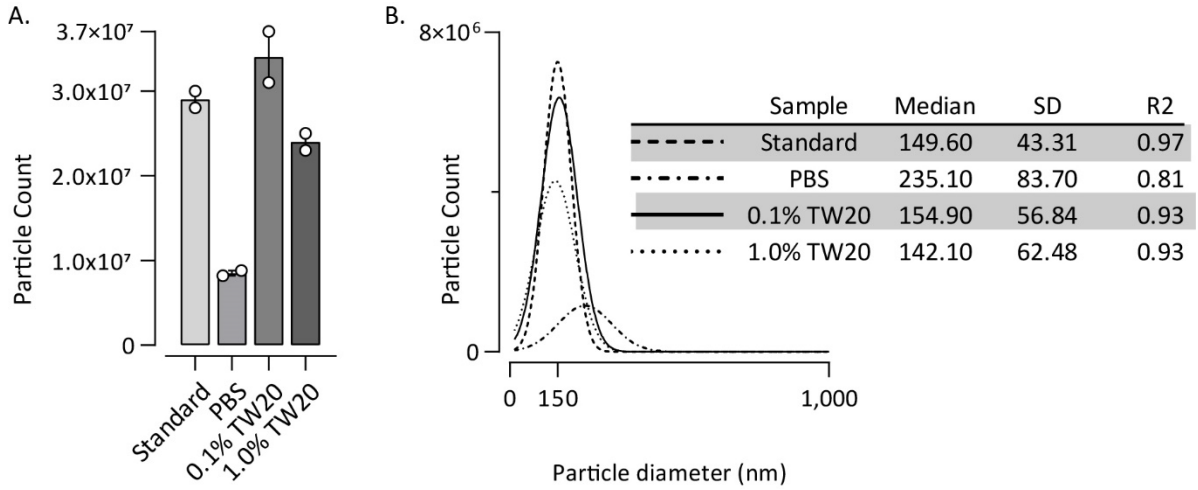

Figure 2: 0.1% TWEEN-20 improves the recovery of rEV material from 300 kDa MWCO filter membranes. A) Absolute particle count from the different recovery strategies using nanoparticle tracking analysis. B) Size distribution of the rEV particles recovered from solution (standard, 149.6 ± 43.3 nm) or from the membrane with PBS (235.1 ± 83.7 nm), 0.1% TWEEN-20 (154.9 ± 56.8 nm) or 1.0% TWEEN-20 (142.1 ± 62.5 nm).

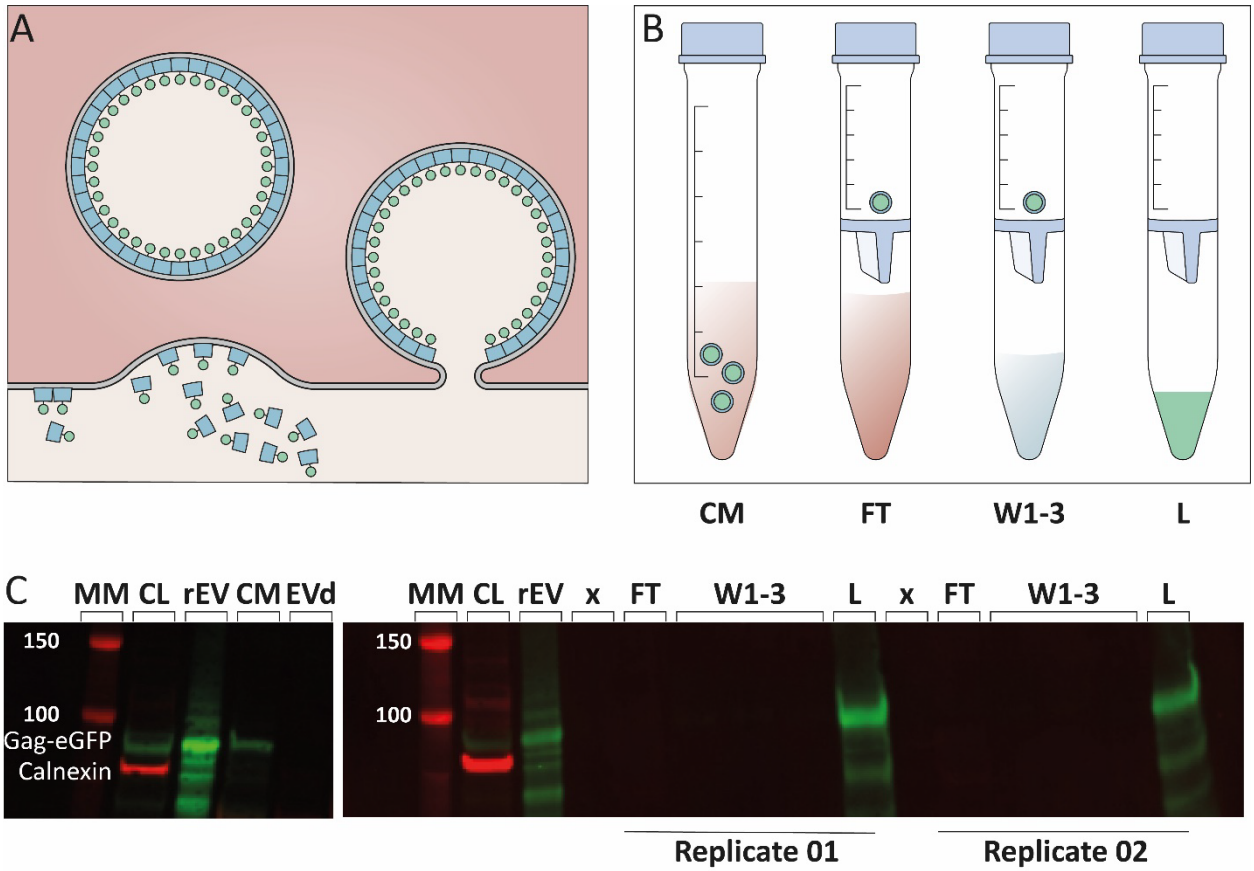

Figure 3: The use of 5% TWEEN-20 in wash buffer has no detrimental effect on the rEV integrity. A) Schematic representation of rEV formation in GAG-eGFP transfected HEK293T cells where the GAG-eGFP fusion proteins assemble at the plasma membrane and induce membrane budding followed by the release of rEV particles into the medium. B) Schematic overview of the rEV enrichment protocol where pre-cleared conditioned medium is diluted twice to a final concentration of 5% TWEEN-20 prior to filtration on a 300 kDa MWCO filter. The retained particles are then washed three times with 5% TWEEN-20 in PBS before recovering the EV proteome by lysing the EVs in 5% SDS. C) Western blot of the individual fractions during rEV enrichment on 300 kDa MWCO filters. Gag-eGFP, a rEV enclosed protein, is absent in both the FT and wash steps, indicating the particles remain intact. The signal is recuperated after lysis, indicating that the strategy of recovering the rEV proteome by immediate lysis using 5% SDS is effective. GAG-eGFP (rEV specific marker; green; app. 85 kDa) and calnexin (ER specific marker; red; app. 80 kDa) are visualized. MM: Molecular weight marker; CL: GAG-eGFP transfected HEK293T cell lysate; rEV: commercial (pure) rEV material; CM: GAG-eGFP transfected HEK293T pre-cleared conditioned medium; EVd: EV depleted FBS; FT: flow-through sample loading (5% TWEEN-20); W1-3: flow-through from wash steps (5% TWEEN-20); L: flow-through after lysis of retained material (5% SDS). X: empty lane.

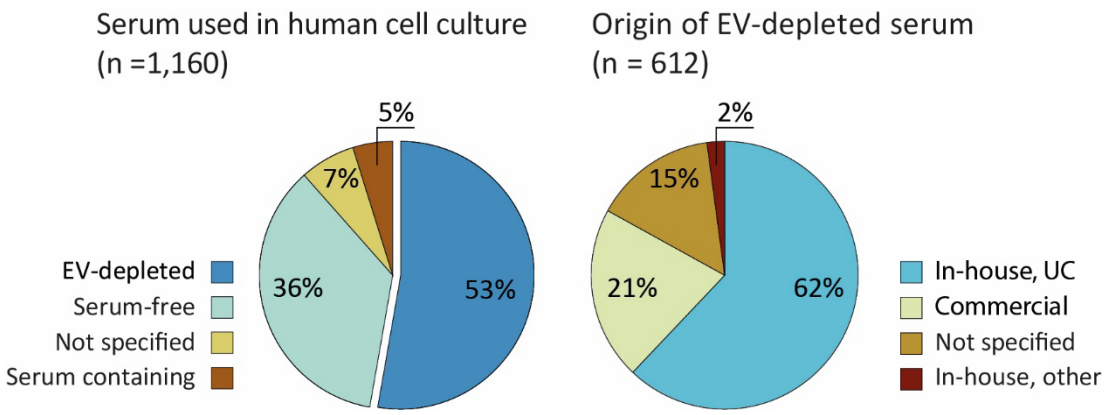

Figure 4: Schematic overview of the use of serum supplementation and its origin in human cell cultures. Over half of the experiments conducted on conditioned medium from human cell cultures used EV-depleted FBS, whereas approximately one third were performed in serum-free conditions. In addition, the origin of EV-depleted FBS is diverse, with over 60% produced by in-house ultra-centrifugation (UC) of standard FBS with differing speeds (min. 100,000 x g) and timeframes (ranging from 2 – 18 h). Data were obtained from EV-TRACK and limited to human cell culture experiments from the period of 2018-2022.

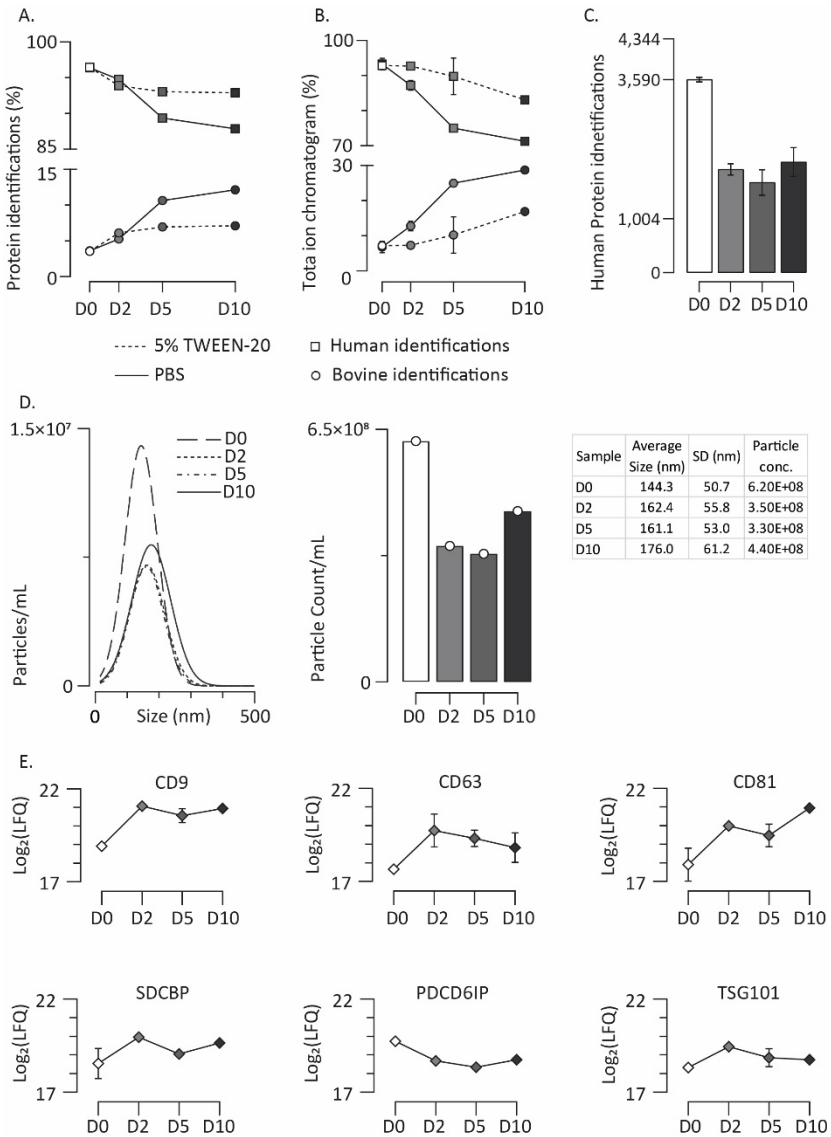

Sample	Average Size (nm)	SD (nm)	Particle conc.
D0	144.3	50.7	6.20E+08
D2	162.4	55.8	3.50E+08
D5	161.1	53.0	3.30E+08
D10	176.0	61.2	4.40E+08

Figure 5: **300 kDa MWCO filtration with 5% TWEEN-20 during wash steps improves the overall purity of the EV samples and allows high recovery of EV proteins**. Supplementing 5% TWEEN-20 to the wash buffer aids in diminishing the precursor intensities from bovine origin compared to those of human proteins (A), thereby reducing the overall number of bovine identifications and increasing the number of human protein identifications (B). C) In total, 4,344 human proteins were identified from the EVs with 1,027 proteins represented across all experiments. Notably, 1,004 proteins were only identified in the 0% EVd FBS conditions. D) The size distribution and EV count across all different experimental conditions. E) Six specific EV protein markers were identified and quantified across all different experiments.

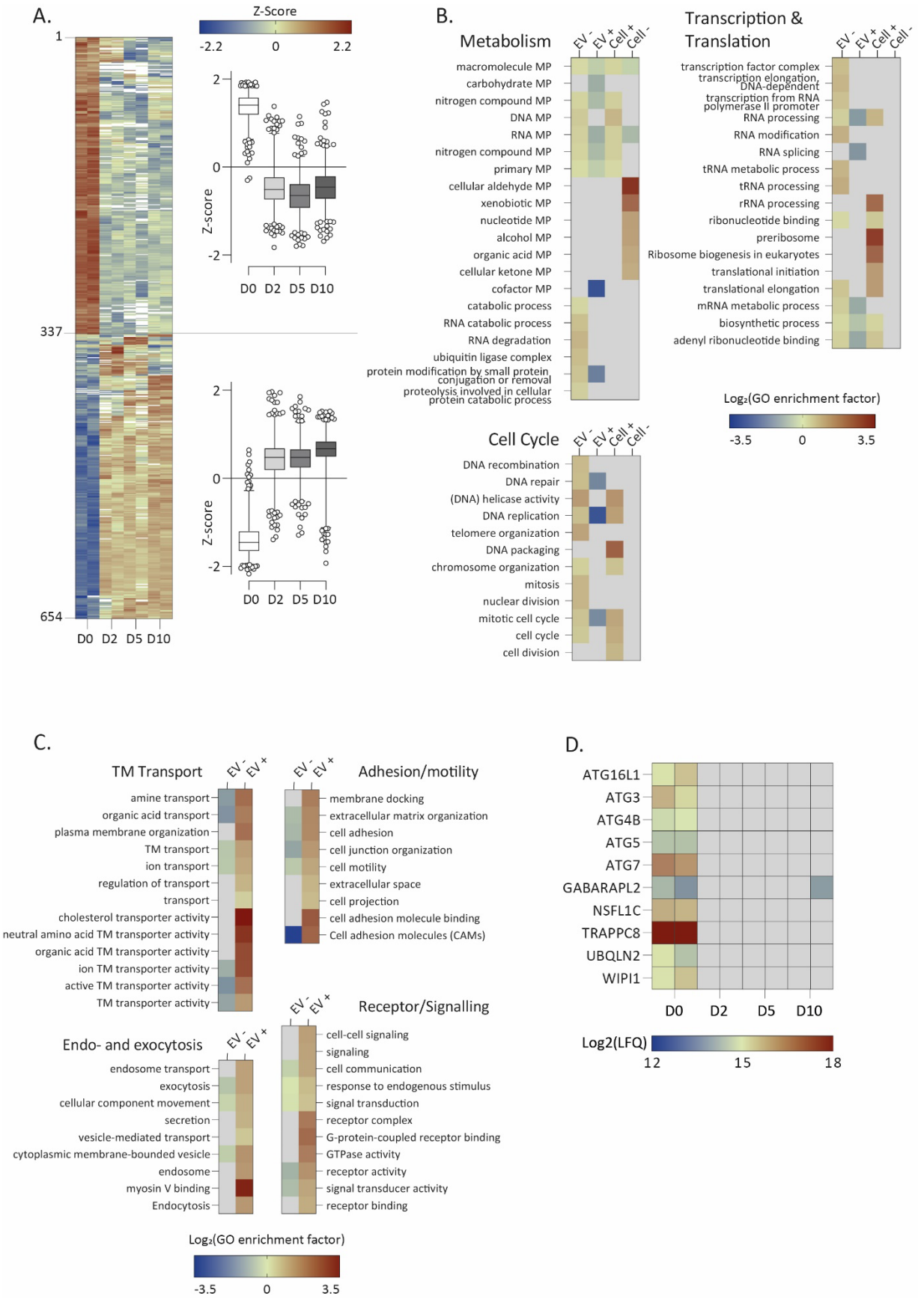
A.
Z-Score
-2.2
0
2.2
1
337
654
D0 D2 D5 D10
Z-score
B.
Metabolism
EV- EV+ Cell+ Cell-
macromolecule MP
carbohydrate MP
nitrogen compound MP
DNA MP
RNA MP
nitrogen compound MP
primary MP
cellular aldehyde MP
xenobiotic MP
nucleotide MP
alcohol MP
organic acid MP
cellular ketone MP
cofactor MP
catabolic process
RNA catabolic process
RNA degradation
ubiquitin ligase complex
protein modification by small protein conjugation or removal
proteolysis involved in cellular protein catabolic process
Transcription & Translation
transcription factor complex
transcription elongation, DNA-dependent
transcription from RNA polymerase II promoter
RNA processing
RNA modification
RNA splicing
tRNA metabolic process
tRNA processing
rRNA processing
ribonucleotide binding
preribosome
Ribosome biogenesis in eukaryotes
translational initiation
translational elongation
mRNA metabolic process
biosynthetic process
adenyl ribonucleotide binding
Log2(GO enrichment factor)
-3.5
0
3.5
Cell Cycle
DNA recombination
DNA repair
(DNA) helicase activity
DNA replication
telomere organization
DNA packaging
chromosome organization
mitosis
nuclear division
mitotic cell cycle
cell cycle
cell division
C.
TM Transport
EV- EV+
amine transport
organic acid transport
plasma membrane organization
TM transport
ion transport
regulation of transport
transport
cholesterol transporter activity
neutral amino acid TM transporter activity
organic acid TM transporter activity
ion TM transporter activity
active TM transporter activity
TM transporter activity
Adhesion/motility
membrane docking
extracellular matrix organization
cell adhesion
cell junction organization
cell motility
extracellular space
cell projection
cell adhesion molecule binding
Cell adhesion molecules (CAMs)
Endo- and exocytosis
endosome transport
exocytosis
cellular component movement
secretion
vesicle-mediated transport
cytoplasmic membrane-bounded vesicle
endosome
myosin V binding
Endocytosis
Receptor/Signalling
cell-cell signaling
signaling
cell communication
response to endogenous stimulus
signal transduction
receptor complex
G-protein-coupled receptor binding
GTPase activity
receptor activity
signal transducer activity
receptor binding
Log2(GO enrichment factor)
-3.5
0
3.5
D.
ATG16L1
ATG3
ATG4B
ATG5
ATG7
GABARAPL2
NSFL1C
TRAPPC8
UBQLN2
WIPI1
D0 D2 D5 D10
Log2(LFQ)
12
15
18

Figure 6: Hierarchical clustering and gene ontology analysis of the EV and cellular proteomes. A) Hierarchical clustering of 654 proteins with a significant differential abundance across the different conditions revealed two main clusters. Legend: Z-scored LFQ intensities B) GO analysis of the EV and cellular proteomes revealed that EVs isolated from serum depleted medium and MCF7 cells from serum containing medium have similar GO terms enriched, contrary to EVs isolated from serum containing medium. The GO terms associated with the upregulated proteome of MCF7 cells cultured in serum depleted medium show a specific enrichment for alternative metabolic pathways. Legend: Log2 transformed GO enrichment factor. C) EVs isolated from serum supplemented medium are significantly enriched for membrane proteins and the associated functions compared to EVs from serum depleted conditions. Legend: Log2 transformed GO enrichment factor. D) Heatmap of autophagy related proteins that were uniquely found in EVs isolated from serum-depleted conditions. Legend: Log2 transformed LFQ values. D0, D2, D5 and D10: DMEM medium supplemented with 0%, 2%, 5% or 10% EVd FBS. EV- & Cell- : EVs and MCF7 cells isolated from serum depleted medium. EV+ & Cell+: EVs and MCF7 cells isolated from serum containing (2%, 5% and 10% EVd FBS) medium. TM: transmembrane. MP: Metabolic process.

Supplementary figures

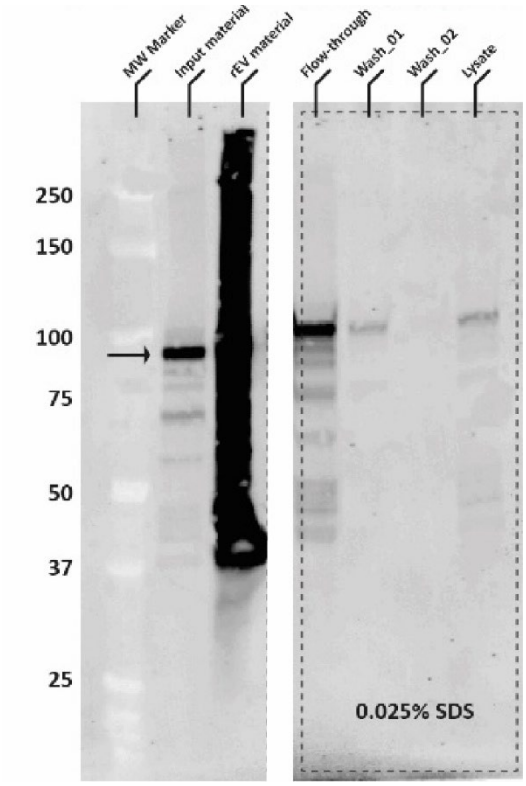

Supplementary Figure 1: Trace amounts of SDS already lyse the bulk of rEV particles in solution. Conditioned medium of GAG-eGFP transfected HEK293T cells was diluted twice to a final concentration of 0.025% SDS in PBS prior to filtration on a 300 kDa MWCO filter. The subsequent washes were done with 0.025% SDS and the retentate was eventually lysed with 5% SDS. The flow-through, wash and lysate fractions were visualized on Western blot using anti-GAG (85 kDa, arrow) and revealed that even at low concentrations, SDS is capable of lysing the bulk of rEV material. MW marker: molecular weight ladder. Input material: pre-cleared conditioned medium from Gag-eGFP transfected HEK293T cells. FT: Flow-through of CM in 0.025% SDS loaded on a 300 kDa MWCO filter. Wash 01 and 02: FT of wash 1 and 2 with 0.025% SDS in PBS. Lysate: FT of the lysate from retained particles with 5% SDS.

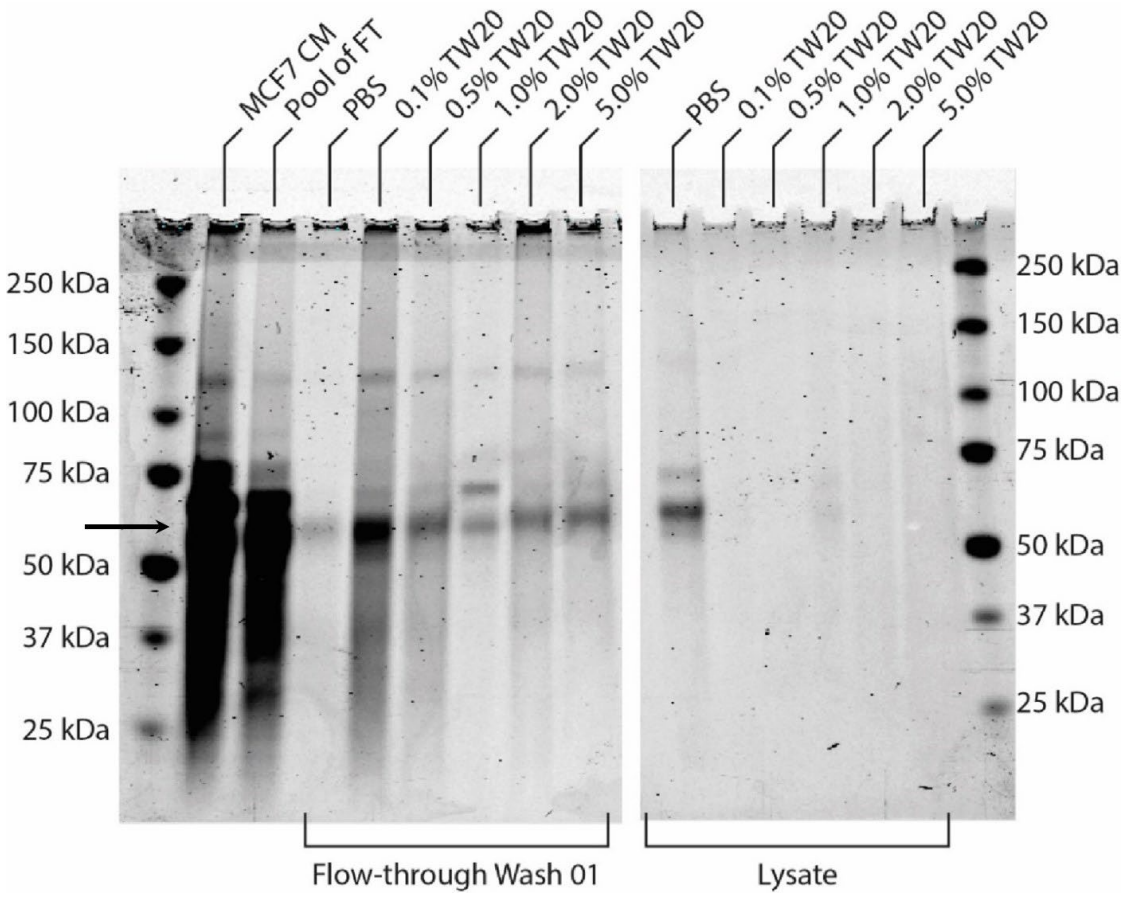

Supplementary Figure 2: Supplementing TWEEN-20 to PBS as wash buffer improves the removal of serum proteins. Pre-cleared MCF7 conditioned medium (CM) was filtered on 300 kDa MWCO filters and washed three times with wash buffers indicated above the gel. The flow-through (FT) from the first wash and the lysate were isolated and loaded on SDS-PAGE, which was stained with Coomassie afterwards to visualize the overall protein material. Focusing on albumin (65 kDa), we observe that PBS is the least capable of removing the bulk of non-EV protein material from the filter, whereas buffers containing TWEEN-20 (TW20) remove more material. In the lysate fractions, we observe an intense 65 kDa band only in the PBS fraction and not in the TWEEN-20 supplemented fractions.

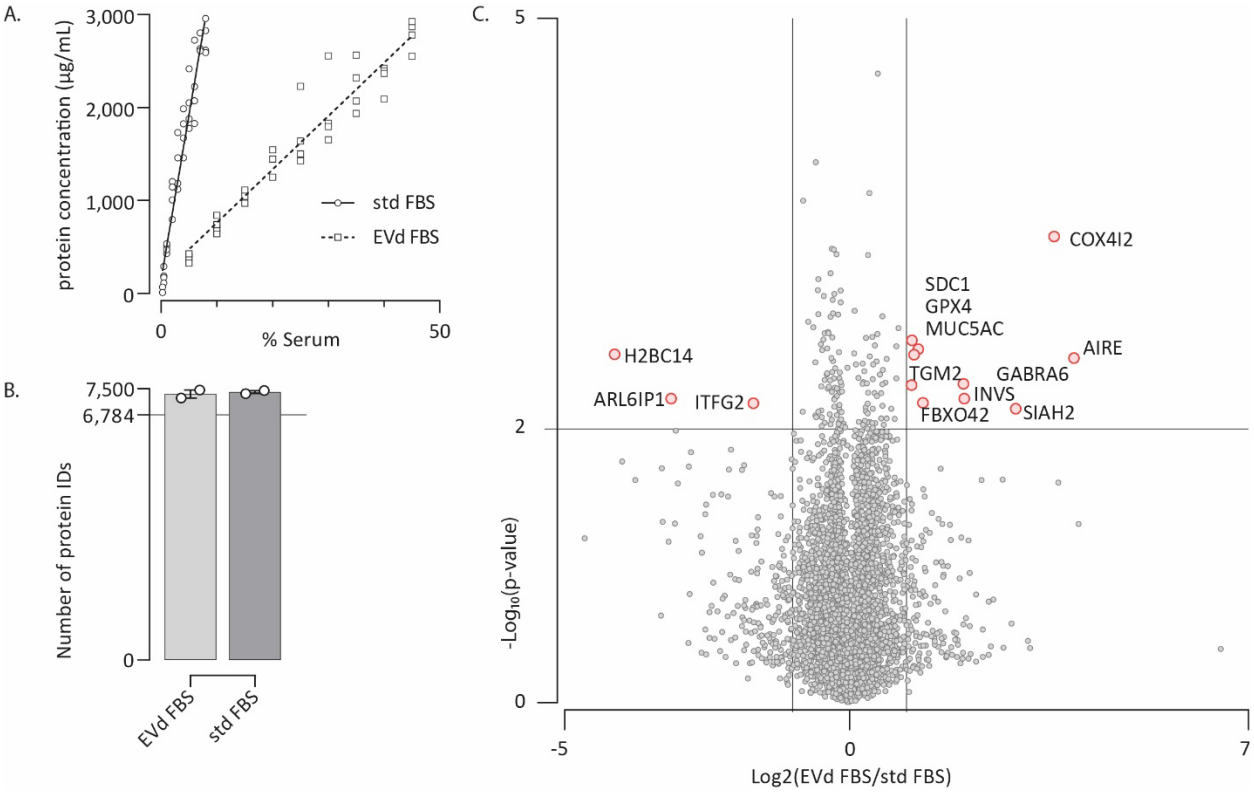

Supplementary Figure 3: Quantitative comparison between the proteomes of MCF7 cells cultured in medium containing 10% EV depleted FBS (EVd FBS) or 10% standard FBS (std FBS). A) EVd FBS contains approximately six times less protein material compared to standard FBS, which might have an effect on the cellular proteome and therefore the EV proteome. B) 8,114 proteins in total were identified from MCF7 cells cultured in either EVd FBS or standard FBS with 6,784 proteins shared between all replicates. C) Quantitative comparison of the individual proteins revealed no major change in the proteome. Only 13 out of 7,579 proteins (0.17% of the proteome) were significantly differentially expressed.

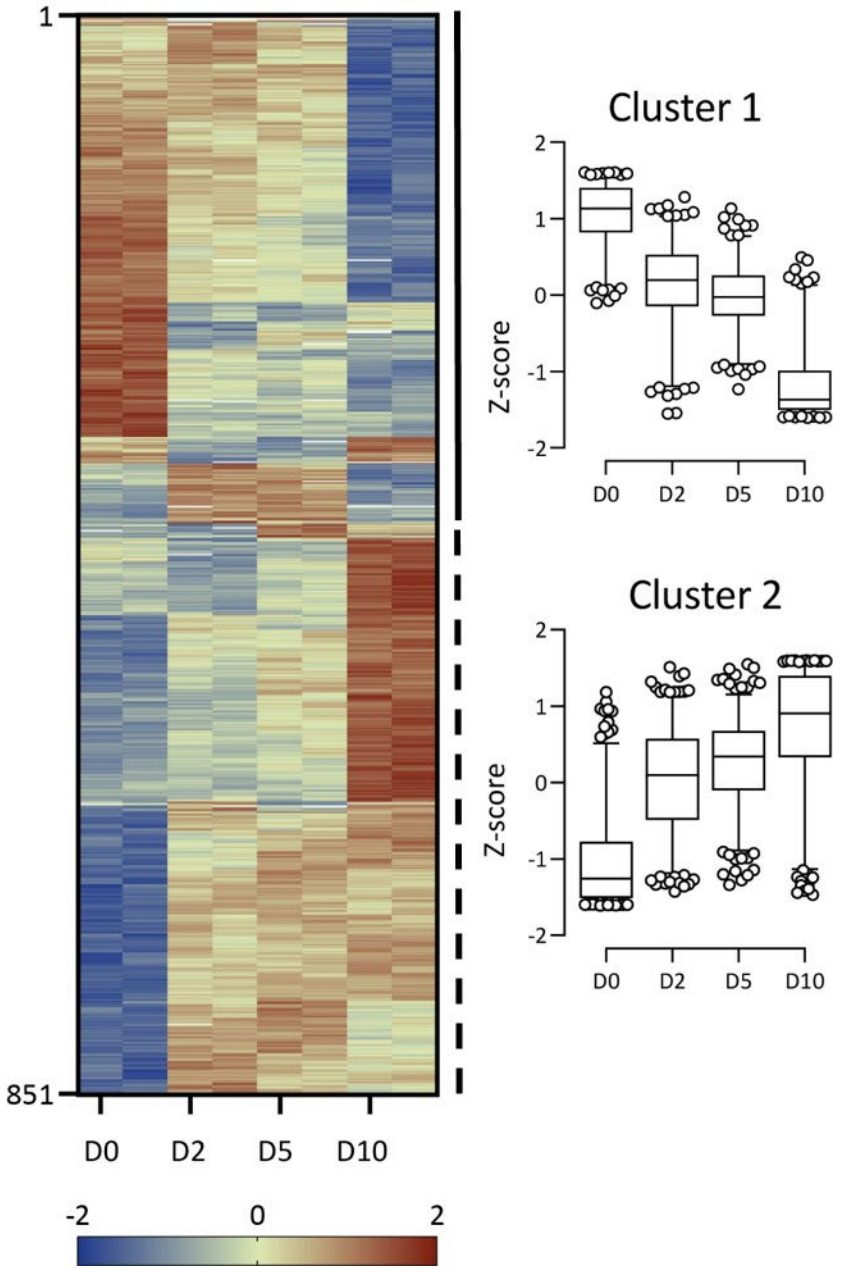

Supplementary Figure 4: Hierarchical clustering of the significant differentially abundant MCF7 cellular proteins between the different conditions. Although more complex to the hierarchical clustering of the EV proteomes, we can distinguish two main clusters; either a decreasing or increasing trend from D0 to D10. Legend: Z-scored log2 transformed LFQ values.

Supplementary data

Protein lists can be found in the supplementary Excel files titled ‘Supplementary data 1 - MCF7 cellular proteome analysis’ and ‘Supplementary data 2 - MCF7 EV proteome analysis’.